 CMES, vol.114, no.3, pp.351-380, 2018

Fast Solving the Cauchy Problems of Poisson Equation in an Arbitrary Three-Dimensional Domain

Cheinshan Liu[1, 2], Fajie Wang[1, 3, *] and Wenzheng Qu[4, *]

Abstract: In this paper we propose a novel two-stage method to solve the three-dimensional Poisson equation in an arbitrary bounded domain enclosed by a smooth boundary. The solution is decomposed into a particular solution and a homogeneous solution. In the first stage a multiple-scale polynomial method (MSPM) is used to approximate the forcing term and then the formula of Tsai et al. [Tsai, Cheng, and Chen (2009)] is used to obtain the corresponding closed-form solution for each polynomial term. Then in the second stage we use a multiple/scale/direction Trefftz method (MSDTM) to find the solution of Laplace equation, of which the directions are uniformly distributed on a unit circle $\mathbb{S}^1$, and the scales are determined a priori by the collocation points on boundary. Two examples of 3D data interpolation, and several numerical examples of direct and inverse Cauchy problems in complex domain confirm the efficiency of the MSPM and the MSDTM.

Keywords: Poisson equation, multiple/scale/direction Trefftz method, multiple-scale polynomial method, irregular domain, inverse Cauchy problem.

1 Introduction

In this paper we propose a new two-stage method to solve the following three-dimensional Poisson equation:

$$\Delta u(\mathbf{x}) = f(\mathbf{x}), \ \ \mathbf{x} \in \Omega \subset \mathbb{R}^3, \tag{1}$$

$$u\Big|_{\mathbf{x}\in\Gamma_1} = g(\mathbf{x}), \tag{2}$$

$$\frac{\partial u(\mathbf{x})}{\partial n}\Big|_{\mathbf{x}\in\Gamma_2} = h(\mathbf{x}), \tag{3}$$

where Δ is the three-dimensional Laplacian operator, Ω is an arbitrary three-dimensional bounded domain enclosed by a smooth boundary Γ, whose normal vector is denoted by

[1] Center for Numerical Simulation Software in Engineering and Sciences, College of Mechanics and Materials, Hohai University, Nanjing 211100, China.

[2] Department of Mechanical and Mechatronic Engineering, National Taiwan Ocean University, Keelung 202-24, Taiwan.

[3] School of Electromechanic Engineering, Qingdao University, Qingdao 266071, China.

[4] Institute of Applied Mathematics, Shandong University of Technology, Zibo 255049, China.

[*] Corresponding author: Fajie Wang. Email: wfj1218@126.com; Wenzhen Qu. Email:quwz@sdut.edu.cn.

$\mathbf{n}$, and $\partial u(\mathbf{x})/\partial n = \nabla u(\mathbf{x}) \cdot \mathbf{n}$. $f(\mathbf{x})$, $g(\mathbf{x})$ and $h(\mathbf{x})$ are given functions. When $\Gamma_1 \cup \Gamma_2 = \Gamma$ and $\Gamma_1 \cap \Gamma_2 = \varnothing$, we encounter a direct problem of the Poisson equation; otherwise, when $\Gamma_1 \cup \Gamma_2 \subset \Gamma$ and $\Gamma_1 \cap \Gamma_2 \neq \varnothing$, we encounter an inverse Cauchy problem of the Poisson equation.

Let $\Gamma_3 = \Gamma_1 \cup \Gamma_2$ and $\Gamma_4 = \Gamma_1 \cap \Gamma_2$. The inverse Cauchy problem of the Poisson equation is specified as follows: Seek an unknown boundary function $F(\mathbf{x})$ on Γ/Γ_3 of the boundary under Eqs. (1-3) with the over-specified data on Γ_4. If the data $F(\mathbf{x})$ are available, then the data $F(\mathbf{x})$, $g(\mathbf{x})$ and $h(\mathbf{x})$ are completed on the whole boundary Γ.

We may consider a mathematical model of the detection of corrosion inside a body, which is a very important technique in engineering application. Given the Dirichlet data $u(\mathbf{x})$ and the Neumann data $u_n(\mathbf{x})$ at the point $\mathbf{x} \in \mathbb{R}^3$ on an accessible part $\Gamma_3 = \Gamma_1 \cup \Gamma_2$ of an irregular boundary, it will be required to solve an inverse Cauchy problem of the Poisson equation to find the unknown function $u(\mathbf{x})$ on an inaccessible part Γ/Γ_3. The inverse Cauchy problem has a wide range of important engineering applications, and thus a large number of publications have been related to it [Chapko and Johansson (2012)].

Liu [Liu (2008a)] has applied a modified Trefftz method (TM) to recover the unknown boundary data for the inverse Cauchy problem, but one needs to consider a regularization technique by truncating the higher-mode components of the given data. Then, Liu [Liu (2008b)] employed the modified collocation Trefftz method with a single characteristic length to solve the inverse Cauchy problems in simply and doubly-connected domains. Liu [Liu (2012b)] has developed a very powerful optimally generalized regularization method to solve the Cauchy problem of Laplace equation by using the method of fundamental solutions (MFS). Up to now, most researches are restricted in the two-dimensional inverse Cauchy problems [Fan, Li and Yeih (2015)]. Only a few studies the inverse Cauchy problem in three- or higher-dimensional cases [Wei, Hon and Cheng (2003); Wang, Chen, Qu et al. (2016)].

There are many papers dealing with the numerical solutions of elliptic type partial differential equations (PDEs). Presently, the method that uses point collocation rather than mesh with weighted integration appears as an effective method, which includes the MFS [Golberg (1995)], the Trefftz method [Li, Lu, Huang et al. (2007); Li, Lu, Hu et al. (2008)] and the radial basis function (RBF) collocation method [Kansa (1990)]. Li et al. [Li, Lu, Hu et al. (2008)] gave a very detailed description of the collocation Trefftz method. The meshless and mesh reduction methods are nowadays the main trend of numerical solution methods of boundary value problems (BVPs) [Liu (2007); Liu (2008b); Pradhan, Shalini, Nataraj et al. (2011); Zhu, Zhang and Atluri (1999); Atluri and Zhu (1998); Atluri, Kim and Cho (1999); Atluri and Shen (2002); Cho, Golberg, Muleshkov et al. (2004); Qu, Chen and Fu (2015); Jin (2004); Li, Lu, Huang et al. (2007)]. Many collocation techniques with the expansion of trial solutions by different basis-functions were employed to solve the elliptic type BVPs; see, for example, [Cheng, Golberg, Kansa et al. (2003); Hu, Li and Cheng (2005); Algahtani (2006); Tian, Reutskiy and Chen (2008); Hu and Chen (2008);

Libre, Emdadi, Kansa et al. (2008)].

In order to overcome the ill-posed linear systems by using the Trefftz method, Liu et al. [Liu, Yeih and Atluri (2009)] have developed a multi-scale Trefftz-collocation Laplacian conditioner. The concept of multi-scale Trefftz-collocation method has been later employed by Chen et al. [Chen, Yeih, Liu et al. (2012)] to solve the sloshing wave problem. Liu et al. [Liu and Atluri (2013)] have employed the concept of equilibrated matrix to find the best multiple-scale of the Trefftz method used in the solution of the inverse Cauchy problems for the Laplace equation, whose resulting linear system is less ill-conditioned.

The meshless methods, however, only solve the homogeneous PDEs. For nonhomogeneous PDEs, a special technique of particular solution is often used to remove the right-hand side, such that the usual MFS, TM and RBF can be applied. It is a key point to find the particular solution of PDEs for the nonhomogeneous problems. The method of particular solution (MPS) is popular in the text book for solving the nonhomogeneous PDEs. In general, we cannot find a global closed-form particular solution for an arbitrary right-hand side. However, for certain function bases, each term in the bases may have a corresponding closed-form particular solution [Cheng (2000); Golberg, Muleshkov, Chen et al. (2003); Chen, Fan and Wen (2012); Lamichhane and Chen (2015)].

In this paper, we will solve the Poisson equation by a two-stage method: first the particular solution and then the Laplace equation by using, respectively, the multiple-scale polynomial method and the multiple/scale/direction Trefftz method. The multiple/scale/direction Trefftz method was first developed by Liu [Liu (2016)] to solve the inverse Cauchy problem of 3D Helmholtz equation, and then Liu et al. [Liu, Qu, Chen et al. (2017)] solved the inverse Cauchy problem of 3D modified Helmholtz equation. This method reducing the number of Trefftz bases for 3D problems is a novel technology, which is not yet applied to solve the inverse Cauchy problem of nonhomogeneous PDE, like the 3D Poisson equation. Besides that, the present paper possesses another novelty by using the multiple-scale technique to interpolate 3D data, which is not yet reported in the literature.

The remainder of this paper is arranged as follows. In Section 2, we introduce a two-stage method and a multiple-scale polynomial method for the interpolation of given data. In Section 3, we find a particular solution, and review the Trefftz method endowing with a set of the Trefftz T-complete bases for the two- dimensional Laplace equation, which is extended to the multi-dimensional Trefftz method for solving the multi-dimensional Laplace equation. In Section 4.1, the numerical examples for the direct problems are given, while the numerical examples for the inverse Cauchy problems are given in Section 4.2. Finally, we draw conclusions in Section 5.

2 A two-stage method

Let $u_p(\mathbf{x})$ be a particular solution of Eq. (1), such that it satisfies

$$\Delta u_p(\mathbf{x}) = f(\mathbf{x}), \quad \mathbf{x} = (x, y, z)^{\mathrm{T}} \in \Omega, \tag{4}$$

but does not satisfy the boundary conditions (2) and (3) necessarily. Hence, the problem (1-3) reduces to solve a homogeneous equation through $u_h(\mathbf{x}) = u(\mathbf{x}) - u_p(\mathbf{x})$:

$$\Delta u_h(\mathbf{x}) = 0, \quad \mathbf{x} \in \Omega, \tag{5}$$

$$u_h\big|_{\mathbf{x}\in\Gamma_1} = g(\mathbf{x}) - u_p(\mathbf{x}), \tag{6}$$

$$\frac{\partial u_h(\mathbf{x})}{\partial n}\Big|_{\mathbf{x}=\Gamma_2} = h(\mathbf{x}) - \frac{\partial u_p(\mathbf{x})}{\partial n}\Big|_{\mathbf{x}=\Gamma_2}. \tag{7}$$

When both $u_h(\mathbf{x})$ and $u_p(\mathbf{x})$ are available, the final solution of Eqs. (1-3) can be obtained by the summation of the particular solution and the homogeneous solution: $u(\mathbf{x}) = u_p(\mathbf{x}) + u_h(\mathbf{x})$.

For an arbitrary function $f(x, y, z)$ it is in general very difficult to obtain a closed-form particular solution, and thus we might find an approximate particular solution. First, we propose a multiple-scale polynomial expansion method to approximate $f(x, y, z)$ by

$$f(x, y, z) = \sum_{i=0}^{M}\sum_{j=0}^{i}\sum_{k=0}^{j} c_{ijk} s_{ijk} x^{i-j} y^{j-k} z^{k}, \tag{8}$$

where c_{ijk} are expansion coefficients with total number being N=(M+1)(M+2)(M+3)/6, and s_{ijk} is a set of multiple-scale to be determined.

First, we set $s_{ijk} = 1$ in Eq. (8). Selecting N_c collocation points in Ω to satisfy Eq. (8) we can obtain a system of linear algebraic equations (LAEs) to solve the N coefficients $\{\alpha_i\} := \{c_{ijk}\}$, which are the vectorization of c_{ijk}. It is convenient to express the resulting LAEs in terms of a matrix-vector product form by

$$\mathbf{A}\alpha = \mathbf{b}. \tag{9}$$

Usually, Eq. (9) is an over-determined system for that we may collocate more points to generate more equations with number N_c, which are used to find N coefficients in α with $N < N_c$. Here the dimension of $\mathbf{A}$ is $N_c \times N$.

The use of the polynomial bases as an interpolation tool to fit the given data is simple and is straightforward to derive the required LAEs to determine the expansion coefficients after a suitable collocation of points in the problem domain. Although the polynomial method in Eq. (8) is derived, which has a drawback that the series diverges when the term $x^{i-j} y^{j-k} z^k$ in Eq. (8) is with a large quantity of x, y and z. In order to obtain a stable and accurate data interpolation, we have to develop a more stable method to solve the resulting LAEs by significantly reducing the condition number.

An equilibrated matrix has either the same norm of all columns or the same norm of all rows, and under this condition the matrix is better-conditioned than that without considering the scaling technique. The problem is the search of some suitable matrices $\mathbf{Q}$ and $\mathbf{P}$, such that the condition number of $\mathbf{QAP}$ is significantly reduced. Liu [Liu (2013)] has proposed a simple procedure to find diagonal $\mathbf{Q}$ and $\mathbf{P}$ only through a few operations.

Liu [Liu (2012a)] has used the concept of equilibrated matrices to choose the best source points for the method of fundamental solutions, while according to the idea of equilibrated matrix, Liu [Liu (2012b)] has developed a general purpose optimally scaled vector regularization method to treat the ill-conditioned linear problems.

The scales are determined below, which are used to reduce the condition number of the new coefficient matrix, such that we can quickly find the expansion coefficients α_i. If the norm of each column of the new coefficient matrix of $\mathbf{B}$ is required to be equal, the multiple-scale $\{s_i\} := \{s_{ijk}\}$, which is obtained from s_{ijk} via a vectorization, is determined by

$$s_i = \frac{R_0}{\|\mathbf{a}_i\|}, \tag{10}$$

where $\mathbf{a}_i$ denotes the ith column of $\mathbf{A}$, and R_0 is a parameter, in general, $R_0 < 1$. Through this simple arrangement, in the new system

$$\mathbf{B}\alpha = \mathbf{b}, \tag{11}$$

the N column norms of the new coefficient matrix $\mathbf{B}$ are all equal to R_0. It can be seen that s_i are fully determined by the collocation points. They can be prepared a priori, upon the collocation points being given.

We can introduce a post-conditioning matrix $\mathbf{P}$ by

$$\mathbf{P} := \mathrm{diag}(s_1, ..., s_N), \tag{12}$$

such that the above equilibrated multiple-scale technique is equivalent to derive the new coefficient $\mathbf{B}$ by

$$\mathbf{B} = \mathbf{AP}, \tag{13}$$

where the dimension of $\mathbf{B}$ is still $N_c \times N$. As $\mathbf{P}$ being a post-conditioner it will render Cond $(\mathbf{B}) \ll$ Cond $(\mathbf{A})$. The scaling technique is used to reduce the ill-conditioned behavior of the resulting LAEs, and in the three-dimensional case the scaling in Eq. (10) is the most easily formulated one.

Instead of Eq. (11), we can solve a normal linear system:

$$\mathbf{D}\alpha = \mathbf{b}_1, \tag{14}$$

where

$$\mathbf{b}_1 := \mathbf{B}^{\mathrm{T}}\mathbf{b}, \mathbf{D} := \mathbf{B}^{\mathrm{T}}\mathbf{B} > 0. \tag{15}$$

The conjugate gradient method (CGM) is a powerful solution scheme and can be employed here to solve Eq. (14), the calculation steps of this method are summarized as follows:

(i) Give an initial value α_0, and then compute $\mathbf{r}_0 = \mathbf{D}\alpha_0 - \mathbf{b}_1$ and set $\mathbf{P}_0 = \mathbf{r}_0$.

(ii) Repeat the following steps for $k = 0, 1, 2, \ldots$,

$$\eta_k = \frac{\|\mathbf{r}_k\|^2}{\mathbf{P}_k^{\mathrm{T}}\mathbf{D}\mathbf{P}_k},$$

$$\alpha_{k+1} = \alpha_k - \eta_k \mathbf{P}_k,$$

$$\mathbf{r}_{k+1} = \mathbf{D}\alpha_{k+1} - \mathbf{b}_1,$$

$$\gamma_{k+1} = \frac{\|\mathbf{r}_{k+1}\|^2}{\|\mathbf{r}_k\|^2},$$

$$\mathbf{P}_{k+1} = \gamma_{k+1}\mathbf{P}_k + \mathbf{r}_{k+1}. \tag{16}$$

Until a given stopping criterion $\|\mathbf{r}_{k+1}\| < \varepsilon$ is satisfied, then stop.

We give two examples for the data interpolation by using the above multiple-scale polynomial method (MSPM).

Examples 1 and 2. We interpolate two given functions:

$$f_1(x,y,z) = 1 + xyz + xy + z^4,$$

$$f_2(x,y,z) = \exp(x+y+z) \tag{17}$$

inside the domain Ω enclosed by a boundary:

$$\Gamma = \{(x,y,z) \mid x = \rho\cos\theta\sin\phi, y = \rho\sin\theta\sin\phi, z = \rho\cos\phi, 0 \le \theta \le 2\pi, 0 \le \phi \le \pi\}, \tag{18}$$

where

$$\rho(\theta,\phi) = (2+\cos\theta)\left[\cos(3\phi) + \sqrt{8-\sin^2(3\phi)}\right]^{\frac{1}{3}}. \tag{19}$$

Under $N_c = 2250$, $N = 35$ ($M = 4$), $R_0 = 0.01$, and $\varepsilon = 10^{-10}$, the CGM is convergent with 65 steps as shown in Fig. 1(a). By comparing the numerical and exact values u(θ) of f_1 on ($r = \rho/2, 0 \le \theta \le 2\pi, \phi = \pi/4$), the maximum error is 1.39×10^{-10} as shown in Fig. 1(b). On the other hand, the maximum error in the whole domain is 1.76×10^{-9}. This example shows that the MSPM is effective and accurate.

Under $N_c = 2250$, $N = 455$ ($M = 12$), $R_0 = 0.01$, and $\varepsilon = 10^{-8}$, the CGM is convergent with 24701 steps as shown in Fig. 2(a). By comparing the numerical and exact values u(θ) of f_2 on ($r = \rho/2, 0 \le \theta \le 2\pi, \phi = \pi/4$), the maximum error is 7.04×10^{-4} as shown in Fig. 2(b).

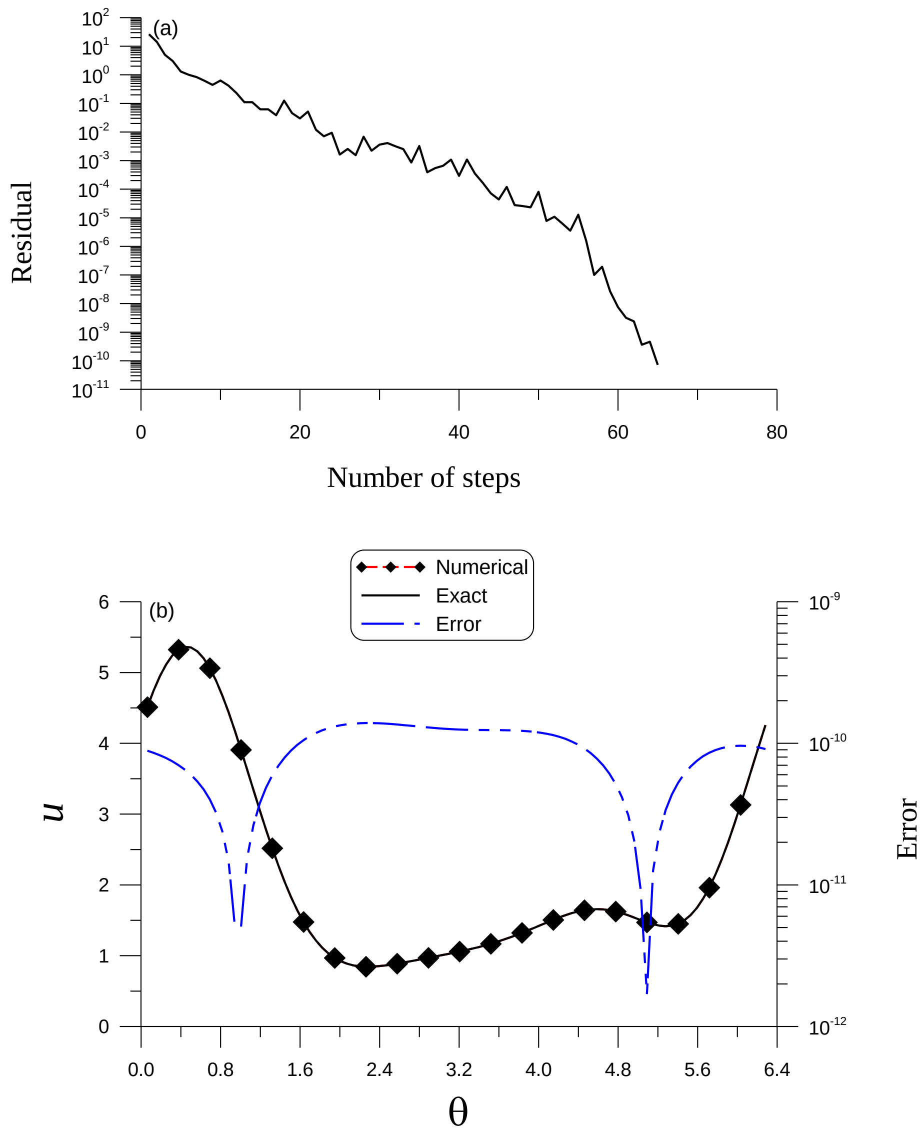

Figure 1: For example 1 of a 3D interpolation in an irregular domain, (a) convergence rate, and (b) the comparison of the numerical and exact solutions. The numerical and exact solutions overlap, such that the difference is not visible in the figure

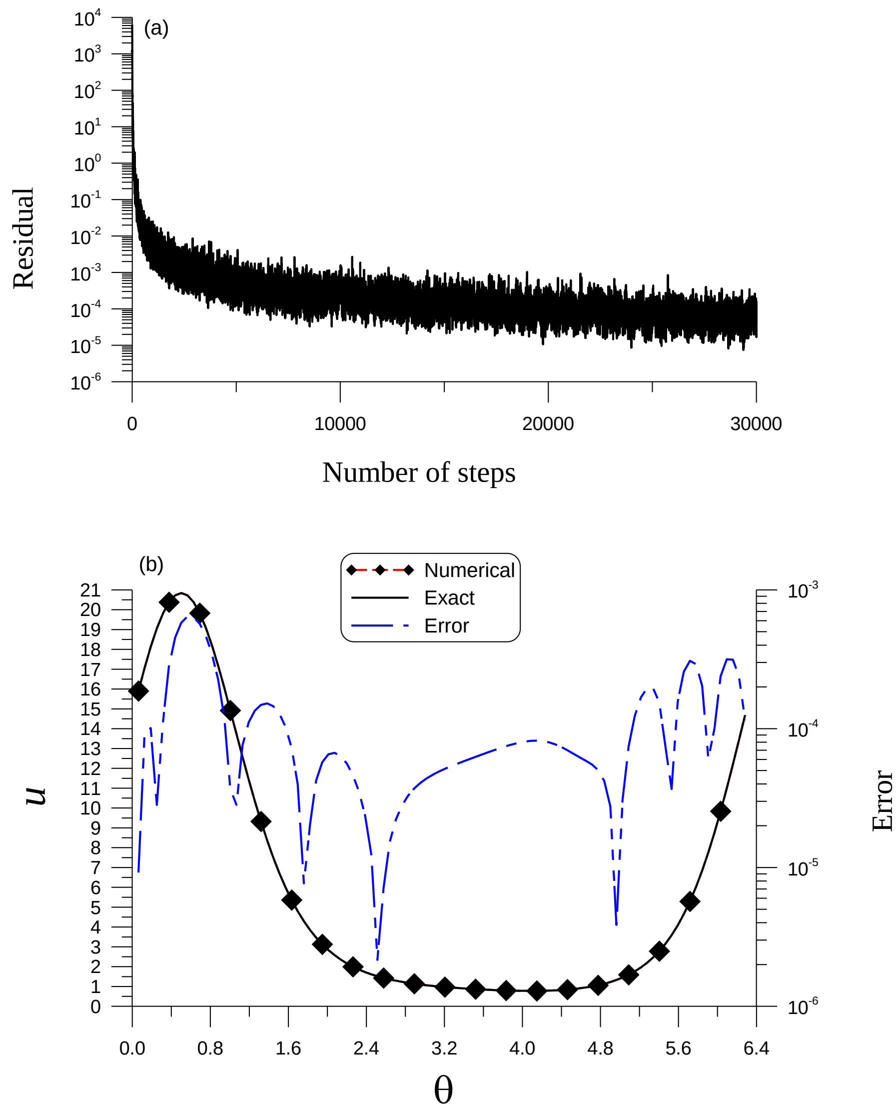

Figure 2: For example 2 of a 3D interpolation of a complex function in an irregular domain, (a) convergence rate, and (b) the comparison of the numerical and exact solutions. The numerical and exact solutions overlap, such that the difference is not visible in the figure

3 A multi-dimensional Trefftz method

3.1 Particular solution

When the interpolation of $f(x, y, z)$ by using Eq. (8) is available, we can get an approximate particular solution $u_p(x, y, z)$ by

$$u_p(x,y,z)=\sum_{i=0}^{M}\sum_{j=0}^{i}\sum_{k=0}^{j}c_{ijk}s_{ijk}F_{i-j,j-k,k}(x,y,z), \tag{20}$$

where $F_{i-j,j-k,k}(x,y,z)$ is given by [Tsai, Cheng, and Chen (2009)]:

$$F_{i-j,j-k,k}(x,y,z)=\sum_{p=0}^{[(j-k)/2]}\sum_{q=0}^{k/2}\frac{(-1)^{p+q}(p+q)!(i-j)!(j-k)!k!x^{i-j+2+2p+2q}y^{j-k-2p}z^{k-2q}}{p!q!(i-j+2+2p+2q)!(j-k-2p)!(k-2q)!}. \tag{21}$$

Although u_p in Eq. (20) is not a closed-form particular solution, but each term in u_p is a closed-form solution. By inserting the above u_p into Eqs. (6) and (7), the right-hand sides can be obtained. Now a remained problem is how to solve Eqs. (5-7).

3.2 The Trefftz method

We first consider the following two-dimensional Laplace equation:

$$\Delta u(x,y)=0,(x,y)\in\Omega, \tag{22}$$

$$u(x,y)=H(x,y),(x,y)\in\Gamma, \tag{23}$$

where Δ is the Laplacian operator, and Γ is the boundary of the problem domain Ω. In terms of

$$(r,\theta)=\left(\sqrt{x_2+y^2},\arctan\frac{y}{x}\right), \tag{24}$$

which are polar coordinates in the Euclidean space $\mathbb{R}^2$, Eq. (22) can be rewritten as

$$\frac{\partial^2 u}{\partial r^2}+\frac{1}{r}\frac{\partial u}{\partial r}+\frac{1}{r^2}\frac{\partial^2 u}{\partial\theta^2}=0. \tag{25}$$

It is well-known that for an interior problem of two-dimensional Laplace equation,

$$\left\{1,r\cos\theta,r\sin\theta,\ldots,r^k\cos(k\theta),r^k\sin(k\theta),\ldots\right\} \tag{26}$$

forms a set of complete Trefftz bases [Liu (2007); Liu (2008b)].

Now, the Trefftz method based on the above bases (26) for the two-dimensional Laplace Eq. (22) can be written as

$$u(x,y)=\sum_{k=1}^{m}\left[a_k r^k\cos(k\theta)+b_k r^k\sin(k\theta)\right]+c_n, \tag{27}$$

where $n=2m+1$ is the number of the unknown coefficients $\{a_k,b_k,c_n\}$, which needs to be determined.

3.3 The multiple-scale-direction Trefftz method

In order to solve the multi-dimensional Laplace equation, we extend the result in Section 3.2 to a multi-dimensional case. Let

$$\mathbf{x} = \left[x_1 ,\dots, x_q \right]^{\mathrm{T}}, \tag{28}$$

where $\mathbf{x}$ denotes the q-dimensional space coordinates. Then the q-dimensional Laplace equation can be written as

$$\sum_{i=1}^{q} \frac{\partial^2 u}{\partial x_i^2} = 0, \tag{29}$$

which is recast to

$$\frac{\partial^2 u}{\partial x_1^2} + \sum_{i=2}^{q} \frac{\partial^2 u}{\partial x_i^2} = 0. \tag{30}$$

Let

$$\mathbf{y} := \left[x_2, \dots, x_q \right]^{\mathrm{T}}, \tag{31}$$

$$\mathbf{d}^j := \left[d_2^j ,\dots, d_q^j \right]^{\mathrm{T}}, \tag{32}$$

$$\eta := \mathbf{d}^j \cdot \mathbf{y} = \sum_{i=2}^{q} d_i^j x_i , \tag{33}$$

where

$$\left\| \mathbf{d}^j \right\|^2 = \sum_{i=2}^{q} \left(d_i^j \right)^2 = 1,\ j = 1,\dots, m_1 . \tag{34}$$

We introduce

$$(r,\theta) := \left(\sqrt{x_1 + \eta^2}, \arctan \frac{\eta}{x_1} \right). \tag{35}$$

As mentioned in Section 3.2 we have the bases

$$B_c^k = r^k \cos k\theta = \left[\sqrt{x_1^2 + \left(\sum_{i=2}^{q} d_i^j x_i \right)^2} \right]^k \cos\left[k \arctan \frac{\sum_{i=2}^{q} d_i^j x_i}{x_i} \right], \tag{36}$$

$$B_s^k = r^k \sin k\theta = \left[\sqrt{x_1^2 + \left(\sum_{i=2}^{q} d_i^j x_i \right)^2} \right]^k \sin\left[k \arctan \frac{\sum_{i=2}^{q} d_i^j x_i}{x_i} \right], \tag{37}$$

which satisfy the two-dimensional Laplace equation in terms of $\left(x_1, \eta \right)$:

$$\frac{\partial^2 B_c^k}{\partial x_1^2} + \frac{\partial^2 B_c^k}{\partial \eta^2} = 0, \tag{38}$$

$$\frac{\partial^2 B_s^k}{\partial x_1^2} + \frac{\partial^2 B_s^k}{\partial \eta^2} = 0 . \tag{39}$$

We can expand the trial solution of $u_h(\mathbf{x})$ by

$$u_h(\mathbf{x}) = \sum_{k=1}^{m}\sum_{j=1}^{m_1} a_{kj} s_{kj}^1 B_c^k + \sum_{k=1}^{m}\sum_{j=1}^{m_1} b_{kj} s_{kj}^2 B_s^k + c_n , \tag{40}$$

where $n = 2mm_1 + 1$ is the number of unknown coefficients $\{a_{kj}, b_{kj}, c_n\}$, and both B_c^k and B_s^k are k-order polynomials of $\mathbf{x}$. In fact, B_c^k and B_s^k are the extensions of $r^k \cos k\theta$ and $r^k \sin k\theta$ in Eq. (26) to the q-dimensional space. It will be proved that B_c^k and B_s^k satisfy the q-dimensional Laplace Eq. (30). Based on the following formula

$$\frac{\partial^2 B_c^k}{\partial x_i^2} = \left(d_i^j\right)^2 \frac{\partial^2 B_c^k}{\partial \eta^2}, i = 2, \dots, q , \tag{41}$$

by summing the above equation with respect to i for $i = 2, \dots, q$, and using Eq. (34), we have

$$\sum_{i=2}^{q} \frac{\partial^2 B_c^k}{\partial x_i^2} = \frac{\partial^2 B_c^k}{\partial \eta^2} \sum_{i=2}^{q} \left(d_i^j\right)^2 = \frac{\partial^2 B_c^k}{\partial \eta^2} . \tag{42}$$

Inserting Eq. (42) into Eq. (38) we have

$$\frac{\partial^2 B_c^k}{\partial x_1^2} + \sum_{i=2}^{q} \frac{\partial^2 B_c^k}{\partial x_i^2} = \frac{\partial^2 B_c^k}{\partial x_1^2} + \frac{\partial^2 B_c^k}{\partial \eta^2} = 0. \tag{43}$$

Thus, it has been proved that B_c^k satisfies the q-dimensional Laplace Eq. (30). Similarly, it can be proved that B_s^k satisfies the q-dimensional Laplace Eq. (30). Considering $\mathbf{d}^j, j = 1, \dots, m_1$ cover m_1 different directions in space, the expansion in Eq. (40) is called a multiple/scale/direction Trefftz method (MSDTM), of which the multiple scales s_{kj}^1 and s_{kj}^2 are determined by the boundary collocation points as that in Section 2.

Ku et al. [Ku, Kuo, Fan et al. (2015)] have employed the multiple-scale Trefftz method with $m_1 = 18$ independent bases of the Bessel functions and the modified Bessel functions expressed in the cylindrical coordinates to solve the three-dimensional Laplacian problems. In detail, it expands the solution by

$$u_h\left(x,y,z\right)=a+bz+\sum_{k=1}^{m=2}\begin{cases}c_{1k}\cosh\left(kz\right)J_0\left(kr\right)+c_{2k}\sinh\left(kz\right)J_0\left(kr\right)\\+c_{3k}\cos\left(kz\right)J_0\left(kr\right)+c_{4k}\sin\left(kz\right)J_0\left(kr\right)\end{cases}$$

$$+\sum_{k=1}^{m_2}\sum_{j=1}^{m_3}\begin{cases}d_{1kj}\cos\left(j\theta\right)\cosh\left(kz\right)J_j\left(kr\right)+d_{2kj}\sin\left(j\theta\right)\sinh\left(kz\right)J_j\left(kr\right)\\+d_{3kj}\cos\left(j\theta\right)\sinh\left(kz\right)J_j\left(kr\right)+d_{4kj}\sin\left(j\theta\right)\cosh\left(kz\right)J_j\left(kr\right)\\+d_{5kj}\cos\left(j\theta\right)\cos\left(kz\right)I_j\left(kr\right)+d_{6kj}\sin\left(j\theta\right)\sin\left(kz\right)I_j\left(kr\right)\\+d_{7kj}\cos\left(j\theta\right)\sin\left(kz\right)I_j\left(kr\right)+d_{8kj}\sin\left(j\theta\right)\cos\left(kz\right)I_j\left(kr\right)\end{cases} \tag{44}$$

$$+\sum_{j=1}^{m_3}\left[e_{1j}r^j\cos\left(j\theta\right)+e_{2j}r^j\sin\left(j\theta\right)+e_{3j}zr^j\cos\left(j\theta\right)+e_{4j}zr^j\sin\left(j\theta\right)\right],$$

where J_0 and J_j are the Bessel functions of the first kind of order zero and j, respectively, and I_0 and I_j are the modified Bessel functions of the first kind of order zero and j, respectively.

It can be seen that the MSDTM is simpler than that of the above standard Trefftz method [Ku, Kuo, Fan et al. (2015)], where many tedious works to establish the bases functions are necessary. When the number of unknown coefficients of MSDTM is $O(mm_1)$, that of the standard Trefftz method is about $O(m_1m_2m_3)$. Later, the above bases have been used to solve the 3D Laplace equation and compared it with the MFS [Lv, Hao, Wang et al. (2017)].

By collocating n_c nodes on the boundary, and considering the boundary conditions (6) and (7), a linear system of equations can be derived to solve the unknown coefficients $\left\{a_{kj},b_{kj},c_n\right\}$ in Eq. (40). Finally, the solution of Eqs. (1-3) can be obtained by:

$$u(x,y,z)=u_p(x,y,z)+u_h(x,y,z), \tag{45}$$

$$u_p(x,y,z)=\sum_{i=0}^{M}\sum_{j=0}^{i}\sum_{k=0}^{j}c_{ijk}s_{ijk}F_{i-j,j-k,k}(x,y,z), \tag{46}$$

$$u_h\left(x,y,z\right)=\sum_{k=1}^{m}\sum_{j=1}^{m_1}a_{kj}s_{kj}^1B_c^k+\sum_{k=1}^{m}\sum_{j=1}^{m_1}b_{kj}s_{kj}^2B_s^k+c_n, \tag{47}$$

where $F_{i-j,j-k,k}(x,y,z)$ is defined in Eq. (21).

4 Numerical tests

Encouraged by the accuracy in the data interpolation, we will further combine the multiple-scale polynomial method and the multiple /scale/direction Trefftz method to solve the Poisson equation, including the direct problem and the inverse Cauchy problems.

4.1 Direct problems

Example 3. First, we consider the Poisson equation as follows:

$$\Delta u = -\sin x - \cos y - \sin z + 6x, (x, y, z) \in \Omega, \tag{48}$$

$$u(x, y, z) = \sin x + \cos y + \sin z + x^3 + x^2 + y^2 - 2z^2, (x, y, z) \in \Gamma, \tag{49}$$

where Ω is a domain with the boundary Γ as shown in Fig. 3, prescribed by the following spherical parametric equation:

$$\Gamma = \{(x, y, z) \mid x = \rho\cos\theta\sin\phi, y = \rho\sin\theta\sin\phi, z = \rho\cos\phi, 0 \le \theta \le 2\pi, 0 \le \phi \le \pi\}, \tag{50}$$

in which

$$\rho(\theta,\phi) = 1 + \frac{1}{8}\sin(10\theta)\sin(9\phi). \tag{51}$$

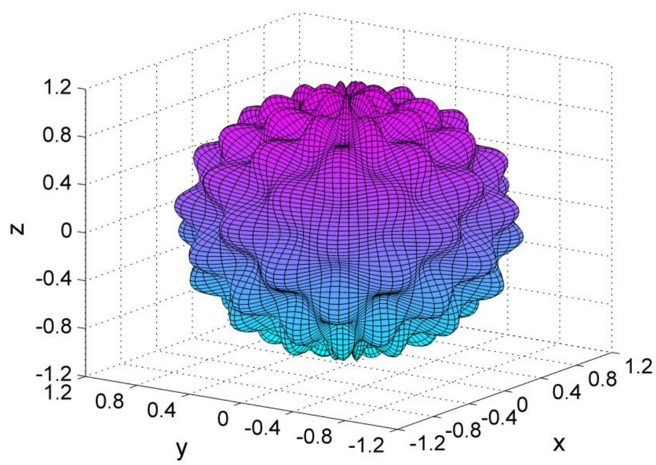

Figure 3: Irregular domain for example 3

The particular solution is obtained by using the MSPM with $N_c = 2744$, $N = 56$ ($M = 5$), $R_0 = 0.0001$, and $\varepsilon = 10^{-10}$. The MSPM is convergent with 75 steps. Then, the homogeneous solution is calculated by using the MSDTM with $n_c = 1600$, $n = 217$, $m = 12$, $m_1 = 9$, and $\varepsilon = 10^{-10}$. As we can see in Fig. 4(a), the MSDTM is convergent with 316 steps. Fig. 4(b) plots the exact and numerical solutions of u on a curve ($r = 2\rho/3, 0 \le \theta \le 2\pi, \phi = \pi/2$), and we can observe that the maximum error is 7.23×10^{-7}. In addition, the maximum error in the whole domain is 7.41×10^{-7}.

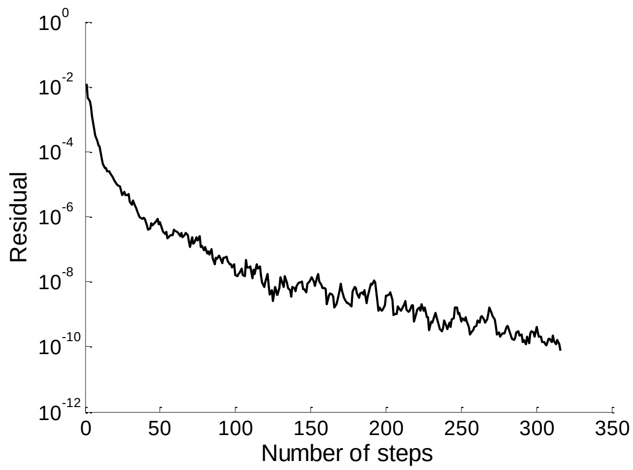

(a)

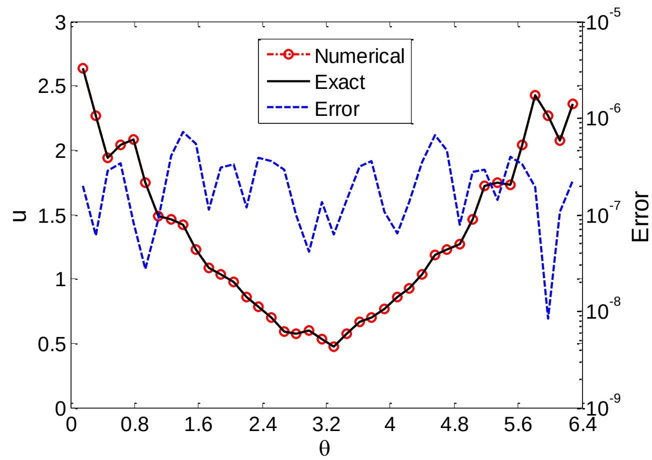

(b)

Figure 4: For example 3 of a 3D Poisson problem in an irregular domain, (a) the convergence rate, (b) the comparison of the numerical and exact solutions

Example 4. In this example we solve a non-harmonic boundary value problem of the Laplace equation, which is still a difficult issue, especially for the three-dimensional problem in an irregular bounded domain. Although the exact solution is not available, the maximum principle is still valid and one can evaluate the maximum error in the whole domain from the maximum error on boundary.

We consider a non-harmonic boundary condition of the Laplace equation:

$$\Delta v(\mathbf{x}) = 0, \ \ \mathbf{x} \in \Omega \subset \mathbb{R}_3, \tag{52}$$

$$v\big|_{\mathbf{x}\in\Gamma} = g(x, y, z) = x^2 y^2 z^2, \tag{53}$$

where $\Delta g \neq 0$. The problem domain is similar to that in Eq. (51); however, we change it to

$$\rho(\theta,\phi) = 1 + \frac{1}{6}\sin(6\theta)\sin(7\phi), \tag{54}$$

in order to compare it with [Lv, Hao, Wang et al. (2017)].

Let

$$u(x,y,z) = v(x,y,z) - g(x,y,z) \tag{55}$$

be a new variable, and then we come to the Poisson equation under a homogeneous boundary condition:

$$\text{Poisson equation: } \begin{cases} \Delta u = f(x,y,z) = -\Delta g(x,y,z), \\ \quad u(x,y,z)\big|_{(x,y,z)\in\Gamma} = 0, \end{cases} \tag{56}$$

where $f(x,y,z) \neq 0$ because $g(x,y,z)$ is a non-harmonic boundary function. When $u(x,y,z)$ is solved we can find $v(x,y,z) = u(x,y,z) + g(x,y,z)$.

We apply the MSPM and MSDTM to solve Eq. (56). For $N_c = 8$, $N = 10$ $M = 2$, $R_0 = 0.01$, $n_c = 2000$, $n = 451$, $m = 15$, and $m_1 = 15$, we apply the MSPM and the MSDTM to solve this problem. The root-mean-square-error (RMSE) at totally 1600 points over the surface is 1.06×10^{-3}, while the maximum error is 3.99×10^{-3}. The accuracy is better than that obtained by Lv et al. [Lv, Hao, Wang et al. (2017)] using the Trefftz method in Eq. (44). They obtained the RMSE to be 2.28×10^{-3} with $n_c = 2000$ and $n = 578$.

In Tab. 1 we list the maximum error (ME) and the RMSE of $v(x,y,z)$ at totally 2500 points on the surface for different m, but other parameters are fixed to be $N_c = 8$, $N = 10$ $M = 2$, $R_0 = 0.01$, $n_c = 3600$, $m_1 = 15$, and $\varepsilon = 10^{-10}$. It can be seen that the MSDTM is convergent.

Table 1: For the non-harmonic boundary value problem of the Laplace equation, comparing the accuracy with different values of m

m	6	8	10	12	14
ME	1.33×10^{-2}	9.24×10^{-3}	5.8×10^{-3}	5.14×10^{-3}	4.20×10^{-3}
RMSE	2.98×10^{-3}	2.45×10^{-3}	1.46×10^{-3}	1.26×10^{-3}	1.07×10^{-3}

In above, it can be seen that the number of collocation points n_c used in the MSDTM is in general much larger than the number of unknown coefficients $n = 2mm_1 + 1$. Because mm_1 is the number of the Trefftz bases used in the numerical solution, it cannot be too large to avoid the highly ill-conditioned behavior of the resultant linear system. On the other hand, in order to match the given boundary conditions accurately, we impose more collocation points to generate more linear equations. Due to these reasons the linear system is usually highly over-determined.

4.2 Inverse Cauchy problems

Before embarking the numerical tests of the presented method to solve the inverse Cauchy problems, we concern with the stability of the MSPM and the MSDTM, in the case when the boundary data are contaminated by the random noise. Thus we investigate the numerical results by adding a different level of random noise on the boundary data:

$$\hat{g}(\theta_{i,}\phi_j) = g(\theta_{i,}\phi_j) + sR(i,\, j),\; \hat{h}(\theta_{i,}\phi_j) = h(\theta_{i,}\phi_j) + sR(i,\, j)\,, \tag{57}$$

where s is the level of noise, and the noise $R(i,\, j)$ are random numbers in [-1, 1].

Example 5. In this example we consider an inverse Cauchy problem of Poisson equation as following:

$$\Delta u = e^x \sin y \cosh z, (x, y, z) \in \Omega\,, \tag{58}$$

$$u(x, y, z) = e^x \sin y \cosh z, (x, y, z) \in \Gamma\,, \tag{59}$$

where Ω is an ellipsoidal vessel with non-uniform thickness with the boundary Γ as shown in Fig. 5. The inner surface of the ellipsoidal vessel is a sphere with a radius $a = 1$. The outer surface is an ellipsoid where the short axis is $b = 1.5$ along the x_3-direction and the long axis $c = 2$ along the x_1-and x_2-directions. The Dirichlet and Neumann boundary conditions are given on the outer surface, while the boundary conditions on the inner surface are not accessible.

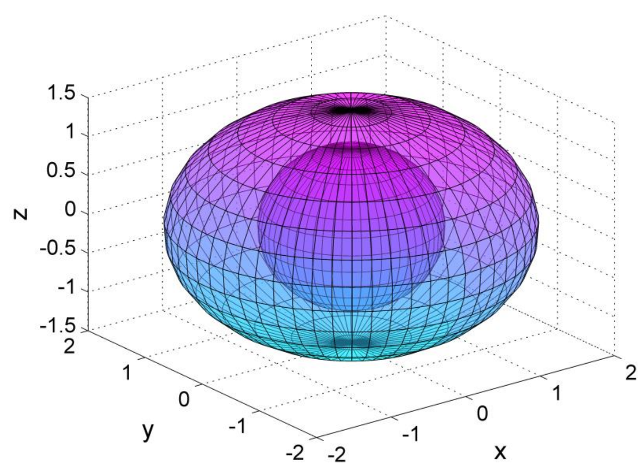

Figure 5: An ellipsoidal vessel with non-uniform thickness, domain for example 5

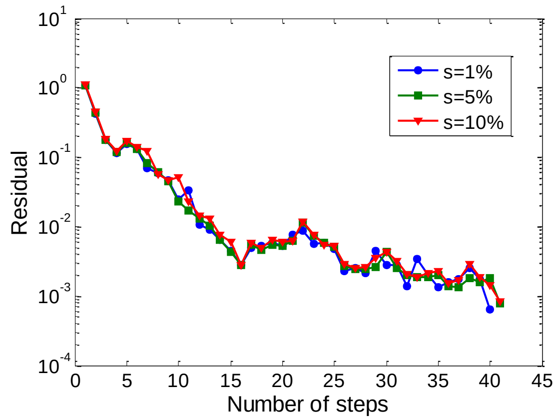

(a)

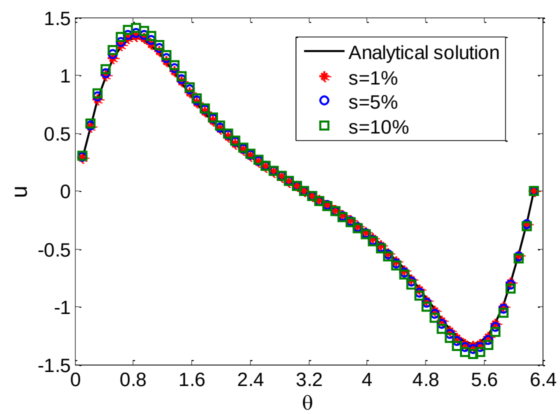

(b)

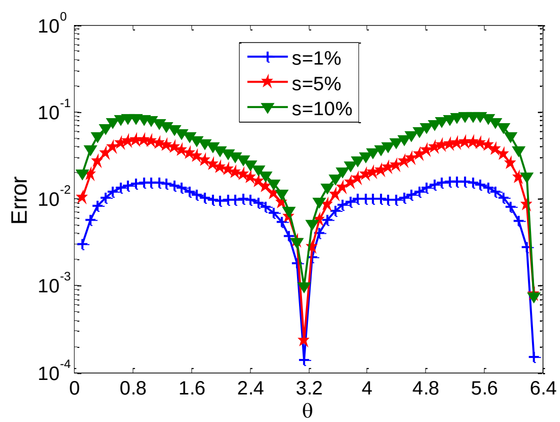

(c)

Figure 6: For example, 5 of a 3D Poisson problem in an irregular domain, (a) the convergence rate, (b) the comparison of the numerical and exact solutions, and (c) the numerical error

In the MSPM with $N_c = 1575$, $N = 56$, $M = 5$, $R_0 = 0.01$ and $\varepsilon = 10^{-3}$, the CGM is convergent with 11 steps. Under $n_c = 1600$, $n = 217$, $m = 12$ and $m_1 = 9$, the MSDTM is convergent with 40 ($s = 1\%$), 41 ($s = 5\%$), 41 ($s = 10\%$) steps under as shown in Fig. 6(a). Figs. 6(b) and (c) present the numerical results and errors for u on $\{(x, y, z) \mid x = a\cos\theta, y = a\sin\theta, z = 0, 0 \le \theta \le 2\pi\}$, obtained by using the MSPM and the MSDTM with various levels of data noise. As shown in these figures, the numerical solutions converge to their corresponding analytical solutions as the amount of noise decreases. Even for a relatively high amount of noise (10%) added into the data, the numerical results still agree quite well to the analytical solution. The maximum error with $s = 10\%$ is 8.18×10^{-2} as shown in Fig. 6(c).

In Tab. 2 we list the ME and the RMSE of u at totally 8000 points in Ω for different m, but other parameters are fixed to be $N_c = 1575$, $N = 56$, $M = 5$, $R_0 = 1$, $\varepsilon = 10^{-3}$, $n_c = 1800$, $m_1 = 10$. It can be seen that the MSDTM is convergent fast and then situates.

Table 2: For example 5 comparing the accuracy with different values of m

m	2	3	4	5
ME	4.23×10^{-1}	1.18×10^{-1}	5.32×10^{-2}	5.29×10^{-2}
RMSE	9.28×10^{-2}	1.94×10^{-2}	1.31×10^{-2}	1.53×10^{-2}

Example 6. In this example we consider the following inverse Cauchy problem of Poisson equation:

$$\Delta u = 6x, (x, y, z) \in \Omega, \tag{60}$$

$$u(x, y, z) = x^3 + x^2 + y^2 - 2z^2, \ (x, y, z) \in \Gamma, \tag{61}$$

where Ω is a torus with the boundary Γ as shown in Fig. 7 prescribed by

$$\Gamma = \left\{(x, y, z) \middle| x = (2+\cos\phi)\cos\theta, y = (2+\cos\phi)\sin\theta, z = \sin\phi\right\}, \tag{62}$$

where $0 \le \theta \le 2\pi, 0 \le \phi \le 2\pi$. In this 3D case, the Dirichlet and Neumann boundary conditions are prescribed on the upper half portion of the torus, while the lower half portion of the torus are under-specified, i.e.

$$u(x, y, z) = g(x, y, z), \tag{63}$$

$$\frac{\partial u(x, y, z)}{\partial n} = \nabla u(x, y, z) \cdot \mathbf{n} = h(x, y, z), \tag{64}$$

where $(x, y, z) = \left((2+\cos\phi)\cos\theta, (2+\cos\phi)\sin\theta, \sin\phi\right), 0 \le \theta \le 2\pi, 0 \le \phi \le \pi$. The normal direction is given by

$$\mathbf{n} = \left[\cos\theta\cos\phi, \sin\theta\cos\phi, \sin\phi\right]^{\mathrm{T}}. \tag{65}$$

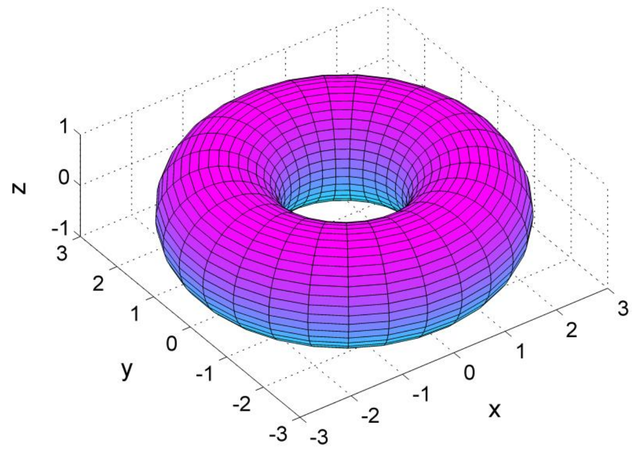

Figure 7: A torus centered at origin, domain for example 6

In the MSPM with $N_c = 3375$, $N = 84$, $M = 6$, $R_0 = 0.001$, and $\varepsilon = 10^{-3}$, the CGM is convergent with 5 steps. Under $n_c = 1600$, $n = 181$, $m = 6$, $m_1 = 15$, the MSDTM is convergent with 16 steps under $\varepsilon = 10^{-3}$ as shown in Fig. 8(a). Fig. 8(b) presents the numerical solutions of u on $\{(x, y, z) \,|\, x = 2\cos\theta, y = 2\sin\theta, z = -1, 0 \le \theta \le 2\pi\}$ obtained by using the MSPM and the MSDTM under $s = 10\%$. It can be observed the numerical solutions are in good agreement with the analytical solution.

Fig. 9 lists the analytical solution and numerical solutions for *u* on lower half portion of the torus with 10% level of data noise. Even for a relatively high amount of noise 10% added into the data, the numerical results still agree quite well with the analytical solution, indicating that the MSPM and the MSDTM yields accurate and stable numerical results for noisy data.

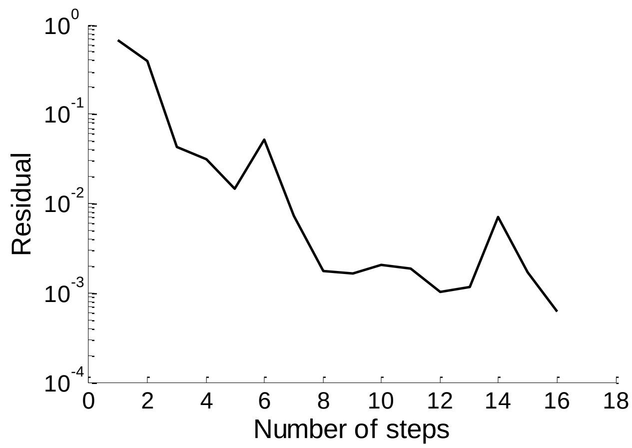

(a)

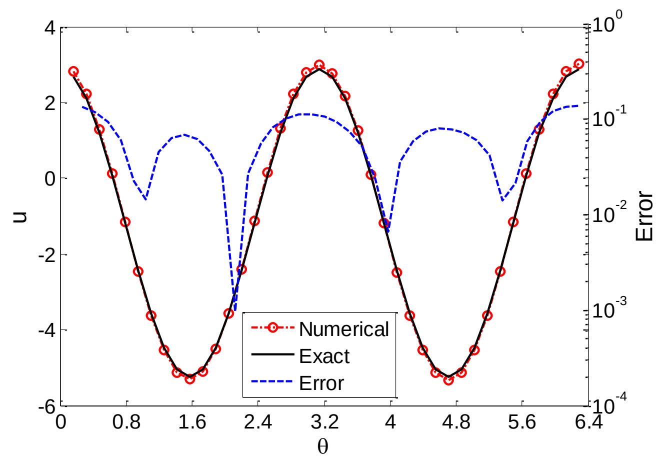

(b)

Figure 8: For example, 6 of a 3D Poisson problem in a torus domain, (a) the convergence rate, (b) the comparison of the numerical and exact solutions. The error reads with respect to the right axis

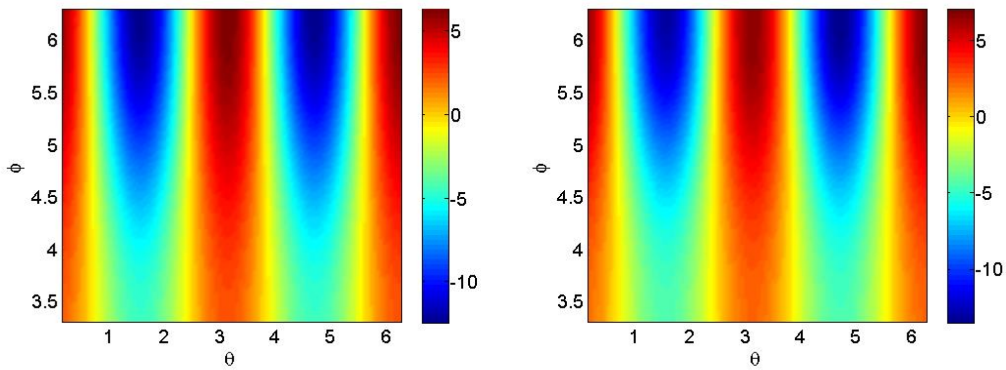

(a) (b)

Figure 9: Distributions of (a) the analytical solutions and (b) the numerical solutions for *u* on the under-specified surface obtained using the MSPM and the MSDTM with *s*=10%

Example 7. We consider the following inverse Cauchy problem of the Poisson equation:

$$\Delta u = -\sin x - \cos y - \sin z,\ (x, y, z) \in \Omega\ ,$$

$$u(x, y, z) = \sin x + \cos y + \sin z, (x, y, z) \in \Gamma\ , \tag{66}$$

where Ω is a peanut-shaped domain with the boundary Γ as shown in Fig. 10, defined by the following parametric equation:

$$\Gamma(x, y, z) = \left\{ x = \rho(\phi)\cos\phi, y = \rho(\phi)\sin\phi\sin\theta, z = \rho(\phi)\sin\phi\cos\theta \right\}, \tag{67}$$

where, $\rho(\phi) = \sqrt{\cos(2\phi) + \sqrt{1.5 - \sin^2(2\phi)}}, 0 \le \theta \le 2\pi, 0 \le \phi \le \pi$.

The Dirichlet and Neumann boundary conditions are over-specified via

$$u(x, y, z) = g(x, y, z), (x, y, z) = \left[\rho(\phi)\cos\phi, \rho(\phi)\sin\phi\sin\theta, \rho(\phi)\sin\phi\cos\theta\right], \tag{68}$$

$$\frac{\partial u(x, y, z)}{\partial n} = h(x, y, z), (x, y, z) = \left[\rho(\phi)\cos\phi, \rho(\phi)\sin\phi\sin\theta, \rho(\phi)\sin\phi\cos\theta\right], \tag{69}$$

in which $0 \le \theta \le \pi, 0 \le \phi \le \pi$.

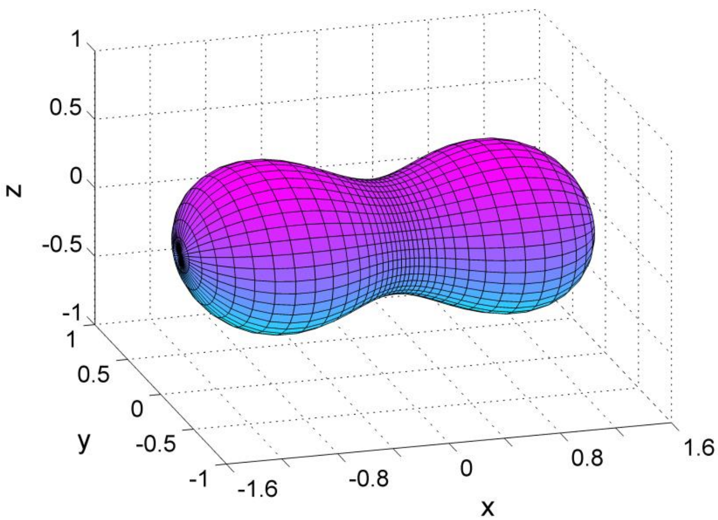

Figure 10: A peanut-shaped domain, domain for example 7

In the MSPM with $N_c = 3375$, $N = 35$, $M = 4$, $R_0 = 0.01$, and $\varepsilon = 10^{-6}$, the CGM is convergent with 21 steps. Under $n_c = 1600$, $n = 49$, $m = 4$, $m_1 = 6$ the MSDTM is convergent with 42 steps under $\varepsilon = 10^{-6}$ as shown in Fig. 11(a). In Fig. 11(b) we compare the numerical and exact solutions of u on the circle $\{(x, y, z) \mid x = \rho(\phi)\cos\phi, y = -\rho(\phi)\sin\phi, z = 0, 0 \le \phi \le \pi\}$, whose maximum error is 7.73×10^{-2} as shown in Fig. 11(b) by dashed-dotted line.

Fig. 12(a) gives the distribution of the analytical solution for u on the under-specified surface. Figs. 12(b-d) show the distributions of the numerical solutions on the under-specified surface obtained by using the MSPM and the MSDTM with $s = 1\%$, $s = 5\%$ and $s = 10\%$ noisy Cauchy data, respectively. As shown in these figures, the numerical results under different noise level are in good agreement with the analytical solution. Furthermore, the numerical solutions converge to the corresponding analytical solutions as the amount of noise decreases. This clearly shows the computational efficiency and accuracy of the proposed numerical scheme. On the other hand, Figs. 13(a-d) display the error surfaces of the numerical results on the under-specified surface, with exact input data, 1% noisy Cauchy data, 5% noisy Cauchy data, and 10% noisy Cauchy data, respectively. It can be seen that, even for a relatively high amount of noise level (10%), the numerical results remain accurate and stable, and converge to the corresponding analytical solution as noise level decreases.

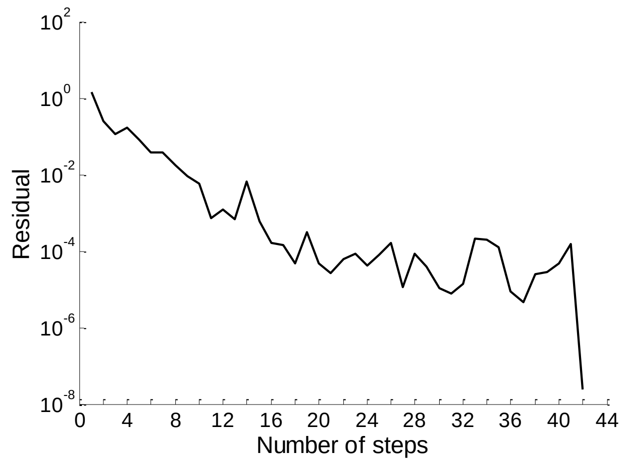

(a)

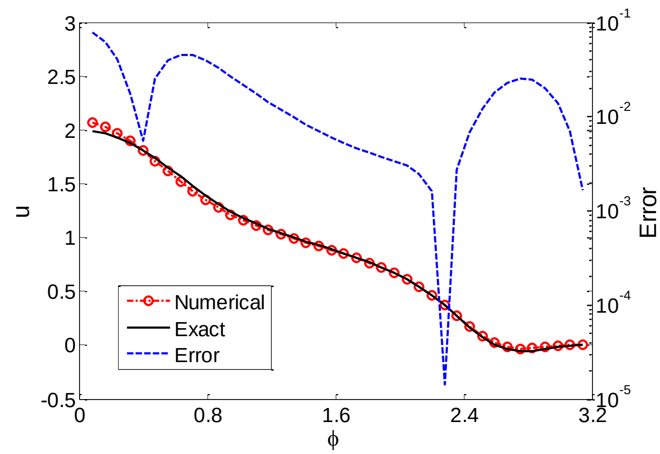

(b)

Figure 11: For example 7 of a 3D Poisson problem in a peanut-shaped domain, (a) the convergence rate of MSDTM, (b) comparing numerical and exact solutions and numerical error. The error reads with respect to the right axis

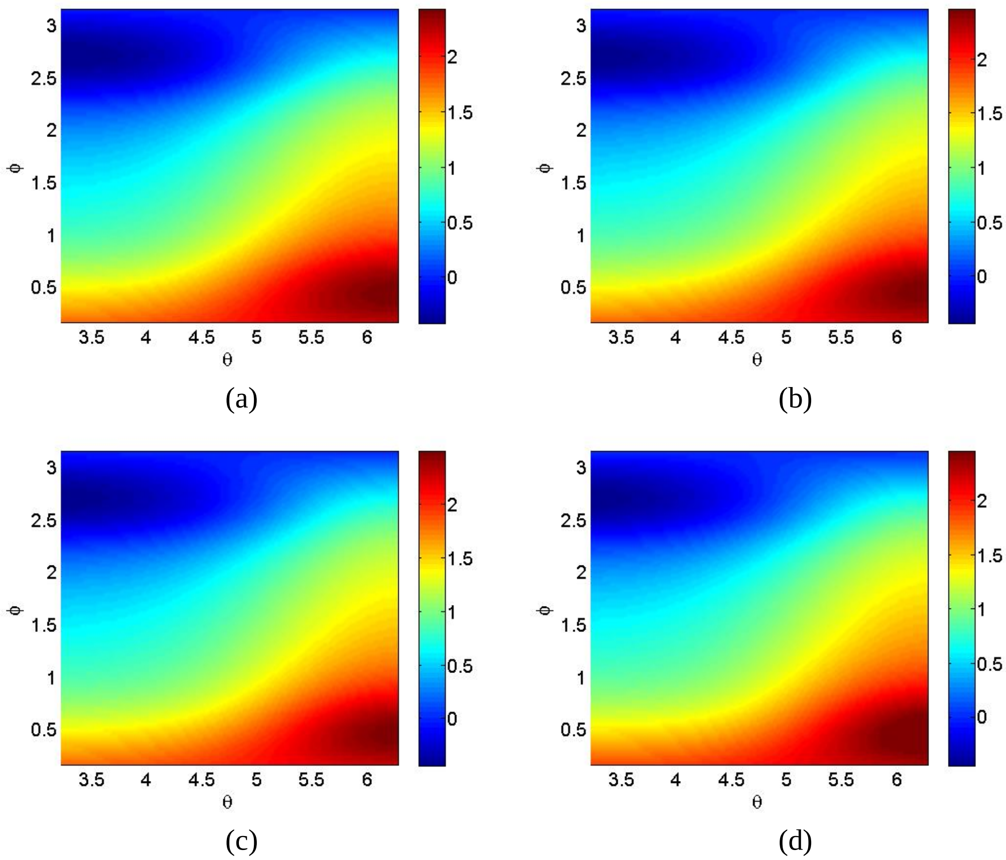

Figure 12: Distribution of (a) the analytical solutions and distributions of the numerical solutions for u on the under-specified surface obtained using the MSPM and the MSDTM with (b) s=1%, (c) s=5% and (d) s=10% noisy Cauchy data

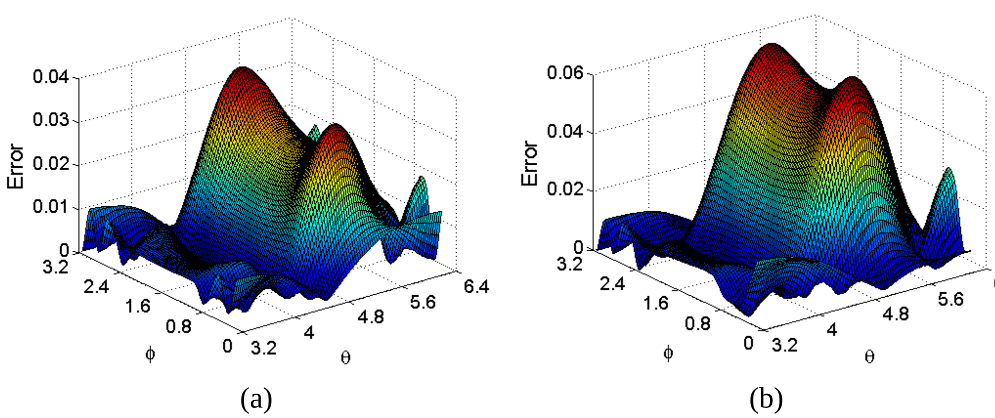

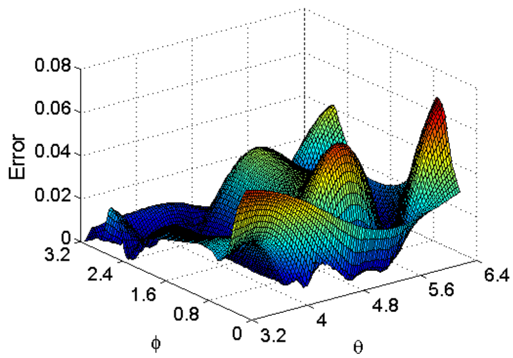

(c)

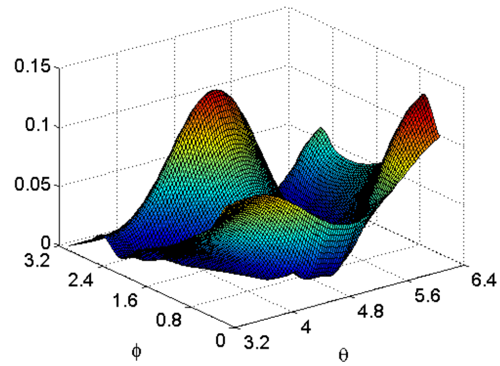

(d)

Figure 13: Error surfaces of u on the under-specified surface obtained using the MSDTM with (a) s=0, (b) s=1%, (c) s=5% and (d) s=10% noisy Cauchy data

Example 8. In this example we consider an inverse Cauchy problem of the Laplace equation in a central hollow sphere [Wang, Chen, Qu et al. (2016)]. The inner and outer radii of the spherical shell are 1 and 2, respectively. The Dirichlet and Neumann boundary conditions are over-specified on the outer surface. The analytical solution is $u = xyz + 10x + 10y + 10z$.

It should be noted that the MSPM is not needed due to the absence of the nonhomogeneous term. To compare with the boundary element method (BEM), Fig. 14 displays the relative error surfaces of the numerical results for the flux on the inner boundary, with exact input data, 1%, 3%, and 5% noisy Cauchy data, respectively. We take $n_c = 1600$, $n = 217$, $m = 9$, $m_1 = 12$, $R_0 = 0.01$, and $\varepsilon = 10^{-8}$. Comparing with Fig. 4 in Wang et al. [Wang, Chen, Qu et al. (2016)], our numerical results are slightly accurate for the various noise level. Furthermore, the proposed method is simpler and faster to implement than the boundary element methods since the MSDTM does not require the time-consuming numerical integrations.

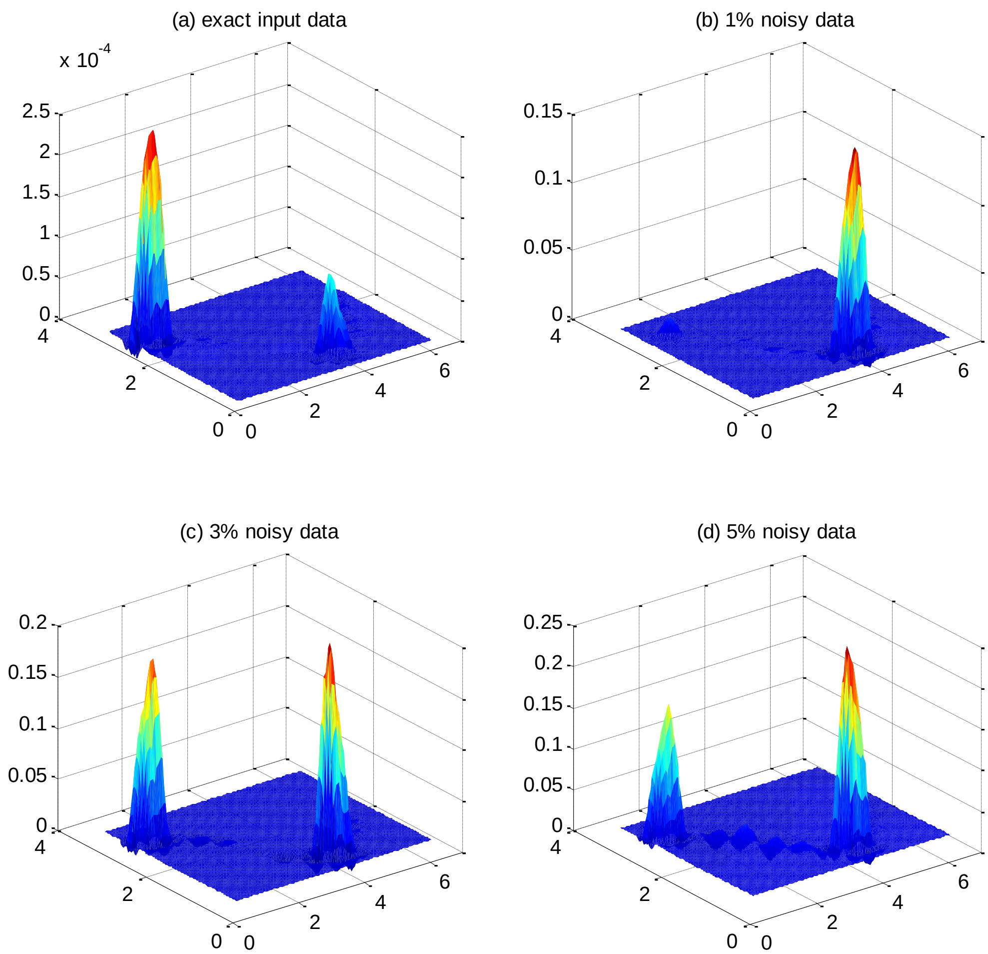

Figure 14: Relative error surfaces of the fluxes on the inner boundary obtained using the MSDTM with (a) exact input data, (b) 1%, (c) 3% and (d) 5% noisy data

Example 9. As the last example we consider an inverse Cauchy problem of the Laplace equation in a torus [Wang, Chen, Qu et al. (2016)], prescribed by the following parametric equation:

$$\Gamma = \left\{(x, y, z) \,|\, x = \rho\cos\theta, y = \rho\sin\theta, z = \sin\phi, 0 \le \theta \le 2\pi, 0 \le \phi \le 2\pi\right\}. \tag{70}$$

In this 3D case, the accessible part of the boundary is specified as

$$\Gamma_1 = \left\{(x, y, z) \,|\, x = \rho\cos\theta, y = \rho\sin\theta, z = \sin\phi, 0 \le \theta \le 2\pi, 0 \le \phi \le 3\pi/2\right\}. \tag{71}$$

In Eqs. (70) and (71), $\rho = 3 + \cos\phi$. The analytical solution of this problem is $u = xy + yz + xz$.

To compare with the boundary element method, Tab. 3 lists the MEs and CPU times of the numerical results on the under-specified surface obtained by using the BEM and the MSDTM with various noisy Cauchy data. In the calculation, the BEM used 48 torus exact elements is in conjunction with the TSVD-GCV regularization technique. In the MSDTM we take $n_c = 1600$, $n = 109$, $m = 6$, $m_1 = 9$, $R_0 = 0.01$, and $\varepsilon = 10^{-8}$. It can be seen from Tab. 3 that the MSDTM is more accurate than the BEM for various noise levels. On the other hand, the BEM requires high amount of CPU time because of expensive numerical integration and regularization.

Table 3: For example 9 comparing the MEs and CPU time by using the BEM and the MSDTM with various noise levels

	Noise level	1%	3%	5%
BEM	ME	3.11×10^{-1}	6.21×10^{-1}	6.15×10^{-1}
	CPU time	106.19	106.09	106.45
MSDTM	ME	5.11×10^{-2}	2.69×10^{-1}	4.07×10^{-1}
	CPU time	0.66	0.67	0.67

5 Conclusions

A simple multiple/scale polynomial method (MSPM) and multiple/scale/direction Trefftz method (MSDTM) were developed for the Poisson equation in an arbitrary three-dimensional (3D) domain. The scales and directions are fully determined by the collocation points and the planar orientations. The proposed method is truly mesh-free and integration-free and its equation system has a small number of unknown coefficients. By using a simple multiple-scale post-conditioner and a simple three-dimensional Trefftz basis, the method can reduce the ill-condition of the resultant linear system. The numerical results demonstrated that the MSPM and the MSDTM is very efficient, even for that adding a large random noise up to 10%.

Acknowledgement: The work described in this paper was supported by the Thousand Talents Plan of China (Grant No. A1211010), the Fundamental Research Funds for the Central Universities (Grant nos. 2017B656X14, 2017B05714), the Postgraduate Research & Practice Innovation Program of Jiangsu Province (Grant No. KYCX17_0487), and the Natural Science Foundation of Shandong Province of China (Grant No. ZR2017BA003).

Reference

Algahtani, H. J. (2006): A meshless method for non-linear Poisson problems with high gradients. *Computer Assisted Mechanics and Engineering Sciences*, vol. 13, no. 3, pp. 367.

Atluri, S. N.; Kim, H. G.; Cho, J. (1999): A critical assessment of the truly meshless local petrov-galerkin (mlpg), and local boundary integral equation (lbie) methods. *Computational mechanics*, vol. 24, no. 5, pp. 348-372.

Atluri, S. N.; Zhu, T. (1998): A new meshless local Petrov-Galerkin (mlpg) approach in computational mechanics. *Computational mechanics*, vol. 22, no. 2, pp. 117-127.

Chapko, R.; Johansson, B. T. (2012): A direct integral equation method for a Cauchy problem for the Laplace equation in 3-dimensional semi-infinite domains. *Computer Modeling in Engineering & Sciences*, vol. 85, pp. 105-128.

Chen, C.; Fan, C.; Wen, P. (2012): The method of approximate particular solutions for solving certain partial differential equations. *Numerical Methods for Partial Differential Equations*, vol. 28, no. 2, pp. 506-522.

Chen, Y. W.; Yeih, W. C.; Liu, C. S.; Chang, J. R. (2012): Numerical simulation of the two-dimensional sloshing problem using a multi-scaling Trefftz method. *Engineering Analysis with Boundary Elements*, vol. 36, no. 1, pp. 9-29.

Cheng, A.; Golberg, M.; Kansa, E.; Zammito, G. (2003): Exponential convergence and hc multiquadric collocation method for partial differential equations. *Numerical Methods for Partial Differential Equations*, vol. 19, no. 5, pp. 571-594.

Cheng, A. D. (2000): Particular solutions of Laplacian, Helmholtz-type, and polyharmonic operators involving higher order radial basis functions. *Engineering Analysis with Boundary Elements*, vol. 24, no. 7, pp. 531-538.

Cho, H. A.; Golberg, M.; Muleshkov, A.; Li, X. (2004): Trefftz methods for time dependent partial differential equations. *Computers, Materials & Continua*, vol. 1, pp. 1-38.

Fan, C. M.; Li, P. W.; Yeih, W. (2015): Generalized finite difference method for solving two-dimensional inverse Cauchy problems. *Inverse Problems in Science and Engineering*, vol. 23, no. 5, pp. 737-759.

Golberg, M.; Muleshkov, A.; Chen, C.; Cheng, A. D. (2003): Polynomial particular solutions for certain partial differential operators. *Numerical Methods for Partial Differential Equations*, vol. 19, no. 1, pp. 112-133.

Golberg, M. A. (1995): The method of fundamental solutions for Poisson's equation. *Engineering Analysis with Boundary Elements*, vol. 16, no. 3, pp. 205-213.

Hu, H.; Chen, J. (2008): Radial basis collocation method and quasi-Newton iteration for nonlinear elliptic problems. *Numerical Methods for Partial Differential Equations*, vol. 24, no. 3, pp. 991-1017.

Hu, H. Y.; Li, Z. C.; Cheng, A. H. D. (2005): Radial basis collocation methods for elliptic boundary value problems. *Computers & Mathematics with Applications*, vol. 50, no. 1, pp. 289-320.

Jin, B. (2004): A meshless method for the Laplace and biharmonic equations subjected to noisy boundary data. *Computer Modeling in Engineering & Sciences*, vol. 6, pp. 253-262.

Kansa, E. J. (1990): Multiquadrics-A scattered data approximation scheme with applications to computational fluid-dynamics-I surface approximations and partial derivative estimates. *Computers & Mathematics with Applications*, vol. 19, no. 8, pp. 127-145.

Ku, C. Y.; Kuo, C. L.; Fan, C. M.; Liu, C. S.; Guan, P. C. (2015): Numerical solution of three-dimensional Laplacian problems using the multiple scale Trefftz method. *Engineering Analysis with Boundary Elements*, vol. 50, pp. 157-168.

Lamichhane, A.; Chen, C. (2015): The closed-form particular solutions for Laplace and biharmonic operators using a Gaussian function. *Applied Mathematics Letters*, vol. 46, pp. 50-56.

Li, Z. C.; Lu, T. T.; Hu, H. Y.; Cheng, A. H. (2008): *Trefftz and collocation methods*. WIT press.

Li, Z. C.; Lu, T. T.; Huang, H. T.; Cheng, A. H. D. (2007): Trefftz, collocation, and other boundary methods-a comparison. *Numerical Methods for Partial Differential Equations*, vol. 23, no. 1, pp. 93-144.

Libre, N. A.; Emdadi, A.; Kansa, E. J.; Rahimian, M.; Shekarchi, M. (2008): A stabilized RBF collocation scheme for Neumann type boundary value problems. *Computer Modeling in Engineering & Sciences*, vol. 24, no. 1, pp. 61-80.

Liu, C. S. (2007): A modified Trefftz method for two-dimensional Laplace equation considering the domain's characteristic length. *Computer Modeling in Engineering & Sciences*, vol. 21, no. 1, pp. 53-65.

Liu, C. S. (2008a): A modified collocation Trefftz method for the inverse Cauchy problem of Laplace equation. *Engineering Analysis with Boundary Elements*, vol. 32, no. 9, pp. 778-785.

Liu, C. S. (2008b): A highly accurate MCTM for inverse Cauchy problems of Laplace equation in arbitrary plane domains. *Computer Modeling in Engineering & Sciences*, vol. 35, no. 2, pp. 91-111.

Liu, C. S. (2012a): An equilibrated method of fundamental solutions to choose the best source points for the Laplace equation. *Engineering Analysis with Boundary Elements*, vol. 36, no. 8, pp. 1235-1245.

Liu, C. S. (2012b): Optimally generalized regularization methods for solving linear inverse problems. *Computers, Materials & Continua*, vol. 29, no. 2, pp. 103-127.

Liu, C. S. (2013): A two-side equilibration method to reduce the condition number of an ill-posed linear system. *Computer Modeling in Engineering & Sciences*, vol. 91, pp. 17-42.

Liu, C. S. (2016): A simple Trefftz method for solving the Cauchy problems of three-dimensional Helmholtz equation. *Engineering Analysis with Boundary Elements*, vol. 63, pp. 105-113.

Liu, C. S.; Atluri, S. N. (2013): Numerical solution of the Laplacian Cauchy problem by using a better postconditioning collocation Trefftz method. *Engineering Analysis with Boundary Elements*, vol. 37, no. 1, pp. 74-83.

Liu, C. S.; Qu, W.; Chen, W.; Lin, J. (2017): A novel Trefftz method of the inverse Cauchy problem for 3D modified Helmholtz equation. *Inverse Problems in Science and Engineering*, vol. 25, no. 9, pp. 1278-1298.

Liu, C. S.; Yeih, W.; Atluri, S. N. (2009): On solving the ill-conditioned system Ax=b: general-purpose conditioners obtained from the boundary-collocation solution of the Laplace equation, using Trefftz expansions with multiple length scales. *Computer Modeling in Engineering & Sciences*, vol. 44, no. 3, pp. 281-311.

Lv, H.; Hao, F.; Wang, Y.; Chen, C. S. (2017): The MFS versus the Trefftz method for the Laplace equation in 3d. *Engineering Analysis with Boundary Elements*, vol. 83, no. 1, pp. 133-140.

Pradhan, D.; Shalini, B.; Nataraj, N.; Pani, A. K. (2011): A Robin-type non-overlapping domain decomposition procedure for second order elliptic problems. *Advances in Computational Mathematics*, vol. 34, no. 4, pp. 339-368.

Qu, W.; Chen, W.; Fu, Z. (2015): Solutions of 2d and 3d non-homogeneous potential problems by using a boundary element-collocation method. *Engineering Analysis with Boundary Elements*, vol. 60, no. 1, pp. 2-9.

Shen, S. N. A. S. (2002): The meshless local Petrov-Galerkin (mlpg) method: a simple & less-costly alternative to the finite element and boundary element methods. *Computer Modeling in Engineering & Sciences*, vol. 3, no. 1, pp. 11-51.

Tian, H. Y.; Reutskiy, S.; Chen, C. (2008): A basis function for approximation and the solutions of partial differential equations. *Numerical Methods for Partial Differential Equations*, vol. 24, no. 3, pp. 1018-1036.

Tsai, C.; Cheng, A. D.; Chen, C. (2009): Particular solutions of splines and monomials for polyharmonic and products of Helmholtz operators. *Engineering Analysis with Boundary Elements*, vol. 33, no. 4, pp. 514-521.

Wang, F.; Chen, W.; Qu, W.; Gu, Y. (2016): A BEM formulation in conjunction with parametric equation approach for three-dimensional Cauchy problems of steady heat conduction. *Engineering Analysis with Boundary Elements*, vol. 63, no. 1, pp. 1-14.

Wei, T.; Hon, Y.; Cheng, J. (2003): Computation for multidimensional Cauchy problem. *SIAM Journal on Control and Optimization*, vol. 42, no. 2, pp. 381-396.

Zhu, T.; Zhang, J.; Atluri, S. (1999): A meshless numerical method based on the local boundary integral equation (lbie) to solve linear and non-linear boundary value problems. *Engineering Analysis with Boundary Elements*, vol. 23, no. 5, pp. 375-389.